

Modelling of Breathing Phenomena within Large Storage Tanks During Rapid Cooling with Ambient Rain

N. Schmidt, J. Denecke, J. Schmidt, M. Davies

Storage tanks in the process industry are often filled with hazardous media under atmospheric conditions. Due to heavy rain showers the tank content is cooled down and the system temperature drops significantly. During this process the pressure decreases and condensate forms. It is known that “vacuum” can cause serious damage on storage tanks due to undersized venting devices. To describe the transient storage tank behaviour modelling of complex inbreathing fluid flow, heat transfer, condensation, retrograde gas states or thermodynamic non-equilibrium is needed. Conservative sizing of protection devices for storage tanks is only possible if the influencing phenomena and their couplings are well understood. The influence of heat transfer through film condensation as an example phenomenon is mentioned by several authors in science and industry, but not included in common models.

With the new approach of ARTEM (advanced reactor and storage tank emission model) phenomena, like condensation or complex heat transfer will be considered for transient vessel venting. Experience and preparatory work have shown that detailed modelling with computational fluid dynamic (CFD) tools is necessary to analyse the complex multiscale phenomena accurately and in sufficient detail. As a first step towards ARTEM, an analytical parameter study on tank breathing with common sizing models and a CFD study on heat transfer through a tank wall is presented.

1 Introduction

Storage Tanks are used in many different sections of industry, e.g. chemical, petrochemical, food industry or agriculture. In these tanks, liquids, gases and mixtures are stored under atmospheric conditions. Many of these tanks are located outdoors and thus exposed to sudden weather changes. The occurrence of temperature variations causes tank venting to compensate volume contraction or expansion of the bulk phase. Common storage tanks buckle at pressure changes of 10 mbars due their relatively thin wall-thickness of 5 mm (Fullarton et al., 1987). To prevent damage, breathing valves (vacuum / pressure valves) are installed on the rooftop to enable inbreathing and outbreathing for non-hazardous tank content. If the content is inflammable or toxic, inert gas blanketing or vapor recovery units are required. For proper sizing of these compensation devices, the ventilation volume flow rate due to weather effects must be considered besides filling or emptying scenarios.

The sizing of venting devices is covered in many standards, like API 2000 (American Petroleum Institute, 2014) or DIN EN ISO 28300 (Deutsches Institut fuer Normung, 2012). The standard models are simplified in a physical and mathematical manner to allow quick manual calculations. Many investigations in literature have shown, that these models are not sufficient for conservative sizing of venting devices (Moncalvo et al., 2016 and Holtkoetter et al., 1997). The basic assumptions of these models are valid only for non-condensable gases. Other tank breathing phenomena, e.g. film condensation, fog formation or convection are excluded. Considering these effects, breathing valves may be significantly undersized (Moncalvo et al., 2016 and Abou-Chakra, 2016).

A sizing method for breathing valves for non-condensable gases was first developed by Nauman in his unpublished report “vacuum and pressure valves on tanks”. Therefore, the maximum inbreathing rate is calculated in dependency of the tank volume. Based on this work and the PTB report “Mathematical estimations of venting operations on roofed-over tanks“ written by Foerster and Schampel in 1979, Sigel et al. (Sigel 1980 and Sigel et al. 1981) developed the extended “Hoechst formula” for non-condensable gases. To validate their model, Sigel et al. performed measurements on a 618 m³ air filled tank. The measured inbreathing volume flow rate was significantly lower than predicted with their calculation model but still an improvement to Naumann. Foerster, Schampel and Steen (Foerster et al., 1984) published a model which was focused on weather dependent breathing phenomena. Their method was not only created for inbreathing predictions but also to calculate outbreathing as a result of temperature rise due to sunshine. Common standards as API 2000 are based on this

work. This model is based on the assumption, that condensation is not a dominant phenomenon in tank breathing and therefore is neglectable. This consideration was revised by several authors in the following years.

Gosslau, Mueller and Weyl (Gosslau et al, 1985) developed a model for thermal tank ventilation including inbreathing and outbreathing. In contrary to Foerster et al., they considered film condensation inside the tank with the conclusion that the impact of condensation on ventilation is not as significant as initially assumed. They validated their model on the measurements of Sigel. Fullarton et al. (Fullarton, 1986) considered film condensation in their inbreathing model. A recognition of this work is, that the Naumann formula leads to significantly oversized venting devices and therefore is too conservative for correct sizing calculations. Based on this knowledge, Fullarton, Evipidris and Schluender (Fullarton et al., 1987) published an extended inbreathing model for condensable vapours. Davies et al. (Moncalvo et al., 2016) applied an enhanced approach to Fullarton's model. They were first to consider the temperature difference between the inflowing air and the bulk phase.

Holtkoetter, Shang and Schecker (Holtkoetter et al., 1997) developed a model that includes film condensation at the tank wall and homogeneous condensation in the vapor space. They validated their model on a tank of 1.18 m³ and concluded, that the submission of condensation heat has a damping effect on cooling of the bulk phase. Salatino, Volepicelli and Volpe (Salatino et al., 1999) introduced a model with regard to the heating process of storage tanks due to sunshine. They compared their results to API 2000 4th edition, Sigel et al. and Naumann. According to their calculations, the API 2000 model underestimates the inbreathing volume flow rate, in contrast to the overestimating Sigel and Naumann model. Vapor condensation was not included in the model but was mentioned as potential source of influence. Abou-Chakra et al. (Abou-Chakra, 2016) validated the implemented calculation model for tank ventilation in the commercial software SuperChems ExpertTM (IoMosaic, 2015). According to their model, venting devices are oversized by up to 60% for non-condensable gases and underestimated by up to 270% for condensable gases using API 2000 6th ed..

The scope of this work is to show, that not only the heat transfer through film condensation has a major impact on tank cooling but also other phenomena like fog formation, convection and flow considerations on the inside. Deeper knowledge about the processes and phenomena inside of tanks is necessary to understand the physical behaviour and to calculate tank ventilation due to weather changes precisely. As first approach towards the overall calculation model ARTEM (advanced reactor and storage tank emission model), a validation of common literature sizing models is presented for condensable and non-condensable contents. In addition, a study on influencing parameter on tank breathing was performed. Further, a two-dimensional CFD simulation of the heat transfer through a tank wall, considering a rain film on the outer surface, is carried out.

The aim of ARTEM in the future is an accurate overall calculation model considering breathing phenomena inside of storage tanks to enable an exact prediction of ventilation flows. Prospectively, the ARTEM model will be extended with the emptying and filling process and additional weather effects, like pressure drop, wind flow or ambient temperature change which need to be considered for the sizing of compensation devices.

2 Phenomena of Storage Tank Cooling

Storage tank venting is caused by thermal pressure changes and load cycles. Regarding thermal changes, two leading scenarios are specified. First, the content of the tank is heated up and second, a hot tank is cooled down by a cooler environment, as depicted in figure 1. This paper focuses on the cooling process with thermal inbreathing which is described below. Other venting phenomena, like pressure changes from a depression, emptying or filling and heating of a tank are not considered in this work but will be in the future. For a proper design of compensation devices, these effects must be considered.

The cooldown of a tank exposed to sun begins when the sun is obscured by clouds with a sudden heavy rain shower. Therein, the ambient temperature drops rapidly and the pressure changes due to the depression. The first raindrops evaporate on the tank wall, causing a local cooldown while the tank wall releases radiant heat. In the course of the shower, the rain intensity may vary over time and the tank is exposed to transient environmental conditions. When wind gusts appear as side effect, a complex wind field is caused, depending on the tank location, that redirects the droplet tracks. Assuming vertical rainfall, the tank roof is covered in droplets. The developing rain film runs down the tank wall and increases the heat transfer significantly. During this process, the film is consistently heated up and partly vaporizes until reaching the ground. Assuming side wind, parts of the shell surface are moistened by forming an unstable rain film. Depending on the surface roughness and environmental conditions, the rain film builds waves until a stable rain film is formed. With rising rain intensity, the film thickness increases and varies over the tank surface. The film velocity accelerates towards the ground and hastens the cooldown of the tank wall. Incoming rain drops suppress the film locally and cause a turbulent mixing of the fluid. With impact on the rain film, the local heat transfer on the surface increases. Some storage tanks are insulated, which can reduce breathing significantly. Thus, due to inhomogeneities in the tank insulation,

wind, sun and rain around the tank, the heat transfer changes locally. To summarize, the heat transfer on the outer tank surface is time- and location-dependent due to rainfall and surface quality.

At the cold tank wall, the boundary layer of gas inside the tank cools down significantly. The density of the cold boundary layer is larger than the density in the middle of the tank and therefore sinks to the tank bottom. By this, convection rolls are formed that increase mixing and mass transfer processes in the tank. The free jet from the inbreathing device acts against the free convection. It depends on the initial bulk fluid and wall temperatures, which ever dominates the flow. Due to wall cooling, the free convection also occurs in the liquid phase. The liquid has a higher heat capacity and cools down more slowly than the gas phase. In addition, the liquid experiences heat transfer through the tank bottom.

Regarding the cool gas boundary layer, a local oversaturation of the gas phase develops and condensate is formed. In the beginning of the condensation process some nuclei stay smaller than the critical drop diameter and vaporize instantaneously. The drop nuclei grow as a result of the cooling conditions to a condensate film, starting at the location with the heaviest subcooling, which is the tank roof. Due to gravity the condensed mass runs down the tank wall to the bottom causing an increase in heat exchange. Depending on the velocity profile, the inside condensate film forms a wavy surface until it is fully stabilized. In some tanks, drops formed on the rooftop are dropping to the bottom when exceeding a critical diameter.

Depending on the stored medium, the gas phase is composed of components with different vapor pressure and diffusion coefficients so that mixing thermodynamics have to be considered in the condensation process. By condensing the gas inside the tank, the mass of the gas phase is reduced and increases the vacuum.

The vacuum is compensated by inbreathing. Wet air loaded with fine particles enters from the environment and cools down the gas at the inlet nozzle. Due to the local oversaturation, heterogeneous condensation on the particle surface and homogeneous condensation, both visible as fog, occur. The associated volume contraction of the tank atmosphere increases the inbreathing airflow. Large aerosol drops sink to the ground, starting a mixing process in the bulk phase that also might accelerate the tank cool-down.

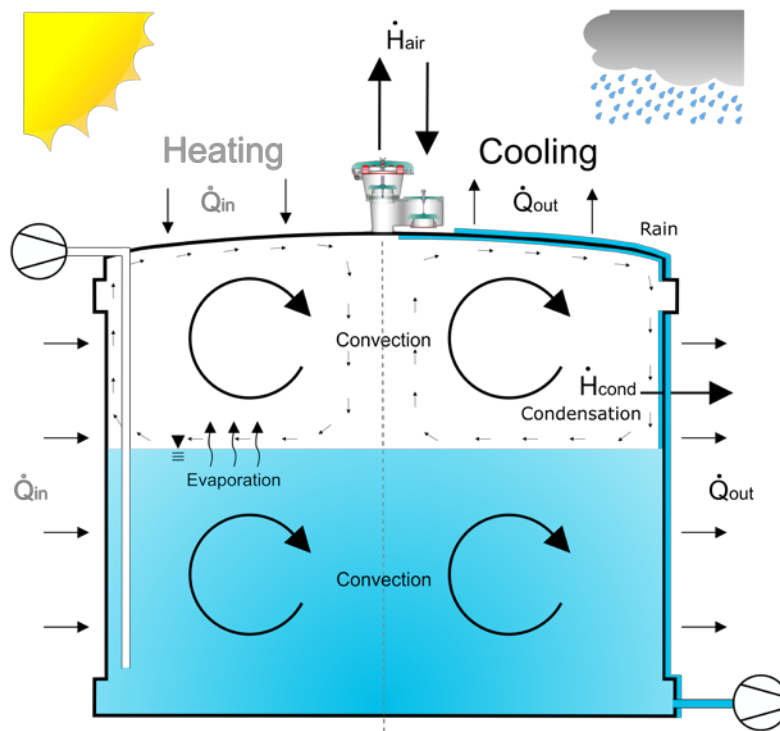


Figure 1. Storage tank venting phenomena to be considered in calculation models.

Most of the phenomena described above are not considered in any model because their interaction is quite complex. To take every phenomenon into account computational fluid dynamics (CFD) is necessary, because the phenomena are not only time but also location dependent. In literature considered effects are heat and mass transfer in the tank, e.g. inbreathing, condensation effects excluding heat conduction through the film, a rain film on the outer surface and heat transfer to the ambience. Momentum effects are entirely neglected.

3 Governing Equations in Common Venting Models

For an accurate calculation of inbreathing, the phenomena described above have to be considered. Thus, common calculation models are governed by many simplifications to economise calculation effort. In the following, a general derivation of governing equations of leading tank venting models for thermal inbreathing is given.

Commonly, the system boundary, as depicted on the right side of Figure 1, is subdivided into four different regions. The first region contains the bulk phase including condensate at the tank wall. The second region is the continuous liquid phase on the bottom of the tank. Region three is governed by the tank wall and the rain film with the environment constitutes region four. In most cases, the liquid phase is neglected because it mitigates the inbreathed air volume flow rate and therefore, the calculation is on the conservative side.

The inbreathing volume flow rate $Q_{v,air}(t)$ is determined by the thermal contraction of the gas phase (Moncalvo et al., 2016; Fullarton, 1986 and Holtkoetter et al., 1997):

$$Q_{v,air}(t) = \frac{V_{bulk}}{T_{bulk}(t)} \frac{dT_{bulk}(t)}{dt} + Q_{v,cond}(t) + Q_{v,cond,sp}(t) \quad (1)$$

Herein, V_{bulk} is the bulk volume, $T_{bulk}(t)$ is temperature of the bulk and $Q_{v,cond}(t)$ is the volume flow rate of the condensate. Holtkoetter et al. (Holtkoetter et al., 1997) also considered homogeneous condensation in their mass balance with an additional term $Q_{v,cond,sp}(t)$. This mass balance is valid for the assumption, that the temperatures of bulk and ambience are equal. Davies extended Fullarton's model among other considerations by assuming different temperatures between bulk and ambience and therefore to take the enthalpy of the inbreathed air into account. By this, the variation of the bulk temperature over time is estimated with an energy balance. The change of internal energy $U_{bulk}(t)$ in the bulk is governed by the enthalpy flux of the inbreathed air $\dot{H}_{air}(t)$, the enthalpy flux of the condensate film $\dot{H}_{cond}(t)$, the enthalpy flux of the spontaneously formed condensate $\dot{H}_{cond,sp}(t)$ and by a heat flux through the tank wall due to the cooler environment $\dot{Q}_{out}(t)$:

$$\begin{aligned} \frac{dU_{bulk}(t)}{dt} &= (M_{cond}(t)c_{p_{cond}} + M_{cond,sp}(t)c_{p_{cond}} + M_{vap}(t)c_{p_{vap}} + M_{air}(t)c_{p_{air}}) \frac{dT_{bulk}(t)}{dt} \\ &= \dot{H}_{air}(t) - \dot{H}_{cond}(t) - \dot{H}_{cond,sp}(t) - \dot{Q}_{out}(t) \end{aligned} \quad (2)$$

Thereby, $M_i(t)$ is the mass of the components described above and c_{p_i} is the specific heat capacity of the components which are assumed to be constant. The enthalpy flux of the inbreathed air is calculated as it follows:

$$\dot{H}_{air}(t) = \rho_{air} Q_{v,air}(t) c_{p_{air}} (T_{bulk}(t) - T_{amb}) \quad (3)$$

With ρ_{air} as air density and T_{amb} as ambient air temperature, both assumed to be constant. The condensation enthalpy flux is:

$$\dot{H}_{cond}(t) = \rho_{cond} Q_{v,cond}(t) \Delta h_{v,cond} \quad (4)$$

Thereby, ρ_{cond} is the constant density of the condensate and $\Delta h_{v,cond}$ is the constant specific condensation enthalpy of the condensate film. The condensation mass flow rate is usually calculated with the Lewis' formula in combination with Antoine's law and the assumption of saturated vapor inside the tank (Moncalvo et al., 2016 and Fullarton et al., 1987). In Holtkoetters model, the enthalpy flux caused by spontaneous condensation is:

$$\dot{H}_{cond,sp}(t) = \rho_{cond} Q_{v,cond,sp}(t) \Delta h_{v,cond} \quad (5)$$

On the basis of their measurements, Holtkoetter et al. determined the volume flow rate of spontaneous condensation $\dot{Q}_{v,cond,sp}(t)$ by means of the proportional aerosol mass fraction. The heat flux leaving the tank is defined by the heat transfer from the bulk to the wall:

$$\dot{Q}_{out}(t) = k_{in}A(T_{bulk}(t) - T_{wall}(t)) \quad (6)$$

The decrease in gas volume due to condensation is included in the mass balance but the heat conduction through the film is neglected in the energy equations in the literature models. Thus, the condensation enthalpy of the film is taken into account.

The tank wall temperature $T_{wall}(t)$ depends on the heat transfer between the bulk phase and the wall k_{in} , the heat transfer between the wall, the rain film k_{rain} and the condensation enthalpy due to the film:

$$M_{wall}c_{p,wall} \frac{dT_{wall}}{dt} = k_{in}A(T_{bulk}(t) - T_{wall}(t)) - k_{rain}A(T_{wall}(t) - T_{rain}(t)) - \rho_{cond}\dot{Q}_{v,cond}(t)\Delta h_{v,cond} \quad (7)$$

The temperature of the rain film $T_{rain}(t)$ is dependent on the rain intensity and the heat transfer to the ambience (Fullarton et al., 1987 and Holtkoetter et al., 1997). In some models, effects like wind cooling, the warm up of the cold rain and tank wall insulation are considered (Moncalvo et al., 2016 and Foerster et al., 1984).

All models mentioned above are derived for single components. For mixtures, there is currently no ventilation model published in literature.

4 Measurements of Inbreathing

Sigel (Sigel et al., 1981) performed measurements on a storage tank with a height of 11.16 m and a diameter of 8.5 m. The tank contained a volume of 618 m³ and was filled up with dry air. During the measurements, the tank was heated up by the sun until a maximum temperature was reached. Afterwards the outer tank surface of 340 m² was cooled down with water from a sprinkler. Thereby, Sigel et al. expected 10% of the water to bounce off the tank wall. In 1980 and 1981 eleven measurements were taken and recorded. The measurements differed in the following points:

- Initial temperature
- Measurement duration
- Temperature of the sprinkle water
- Temperature difference between the initial and end temperature

Despite these differences, the temporal progression of the graphical measurement display was quite similar. The maximum inbreathing volume flow rate over all measurements was situated between 71 m³/hr and 114 m³/hr. The size of the tank was sufficient to illustrate a realistic cooling scenario but with a maximum sprinkling intensity of 69 kg/m²hr, only rain showers to occur every second year on average were simulated (Sigel et al. 1983). Foerster et al. (Foerster et al., 1984) considered rain showers to occur every 100 years on average with an effective rain intensity of 143.7 kg/m²h. Unfortunately, information is missing to simulate the realistic setup, e.g. the exact measurement day time, the ground temperature, the temperature and moisture level of the inbreathed air, wall temperature in the beginning, property data of the tank wall and a reliable technical drawing of the tank.

Holtkoetter (Holtkoetter et al., 1997) performed measurements on a 1.18 m³ laboratory tank. The bulk phase was heated up to 328 K and cooled down by 40 K. The cooling was accomplished with a sprinkler mounted on top of the tank which produced a rain flow intensity of 10 kg/m²h, according to Abou-Chakra (Abou-Chakra, 2016). The measurements were conducted with three different media inside the tank: water, methanol and isopropanol. Holtkoetter observed besides film condensation also fog formation in the tank through small windows in the tank wall. The liquid mass of the spontaneously condensed aerosol phase was measured with a filter module. Before and after the measurements the mass of the filter was weighted to determine the amount of homogeneous condensate. The highest inbreathing rate was observed in the methanol measurements. During the water measurements, 22% of the overall condensation mass was associated to fog formation, where only 9% of spontaneous condensation mass occurred during the measurements with methanol. The fog formation has a damping effect on the cooldown, due to the emission of condensation heat. Because the measurements were performed on a laboratory tank, the observation of Holtkoetter should be reproduced on a large tank to evaluate the scale up effects. In addition, information about the exact measurement conditions is missing, e.g. the

properties of the tank material, the rain temperature and intensity, the location and size of the breathing device and a technical drawing of the tank. Without this information an accurate simulation of the measurements is not possible. These uncertainties are considered in the subsequent validation of the literature models.

5 Comparison of Measurements and Models for Inbreathing

In the following, three relevant inbreathing models are compared to the measurements described above: the model of Fullarton et al. (Fullarton et al., 1987) and Davies et al. (Moncalvo et al., 2016) which both are based on the model of Foerster et al. (Foerster et al., 1984). While Foerster did not consider condensation as governing effect of tank breathing, Fullarton derived a model with condensation as significant parameter. This model was extended by Davies. The models are based on the equations and assumptions described in chapter 3.

The validation of the models on the Sigel measurements, relies on the following assumptions: A steel tank with a height of 8.5 m and a H/D-ratio of 0.8 was used. The tank atmosphere was exclusively filled with air. An inner heat transfer coefficient of $5 \text{ W/m}^2\text{K}$ (bulk to wall), a liquid heat transfer coefficient of $5000 \text{ W/m}^2\text{K}$ (wall to rain film) and an outer heat transfer coefficient of $25 \text{ W/m}^2\text{K}$ (rain film to ambience) were considered. The tank wall thickness was assumed to be 5 mm.

Compared to the measurements of Sigel et al. (Sigel et al. 1981) from 9th July, 1981, the calculation with the Foerster model shows a discrepancy of 43%, see Figure 2. A weakness of the Foerster model is the assumption that film condensation and fog formation are not of significant importance on influencing the inbreathing rate. This statement was revised by Fullarton et al. (Fullarton et al., 1987). Therefore, the data of Sigel are mirrored with an accuracy of 1% by Fullarton's model and Davies' model. The two curves coincide exactly in figure 2.

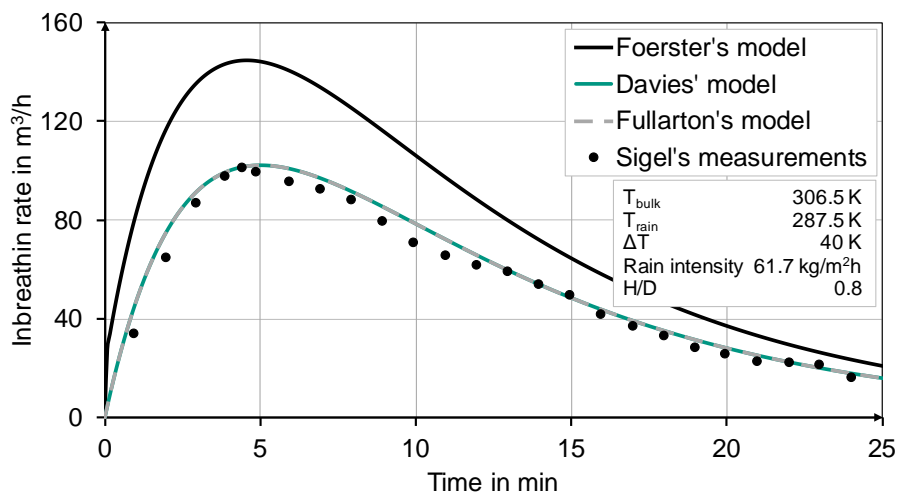


Figure 2. Inbreathing models of Foerster (Foerster et al., 1984), Davies (Moncalvo et al., 2016) and Fullarton (Fullarton et al., 1987) for non-condensable gases compared to Sigel's measurements (Sigel et al. 1981).

However, a critical error consideration of the measurement data is not negligible. Sigel assumed in his measurements that 10% of the water sprayed onto the tank rebounds from the tank surface and therefore does not contribute to cooling the surface. This assumption has not been verified. In addition, the breathing of the tank was facilitated by a long supply line. The pressure loss in this supply line is not known. Finally, weather information is incompletely listed in the experimental protocols, e.g. data on humidity, solar radiation or wind influences are missing.

A contrary situation occurs by the comparison of the models for condensable vapours to the measurement of Holtkoetter. Therefore, a steel tank with a height of 1,5 m and a H/D-ratio of 1.5 was used. The tank atmosphere was assumed to be saturated with vapor, the liquid inside the tank was neglected. An inner heat transfer coefficient of $5 \text{ W/m}^2\text{K}$ (bulk to wall), a liquid heat transfer coefficient of $5000 \text{ W/m}^2\text{K}$ (wall to rain film) and an outer heat transfer coefficient of $25 \text{ W/m}^2\text{K}$ (rain film to ambience) were considered.

In Figure 3, Holtkoetter's measurements for water compared to Davies' and Fullarton's model are displayed.

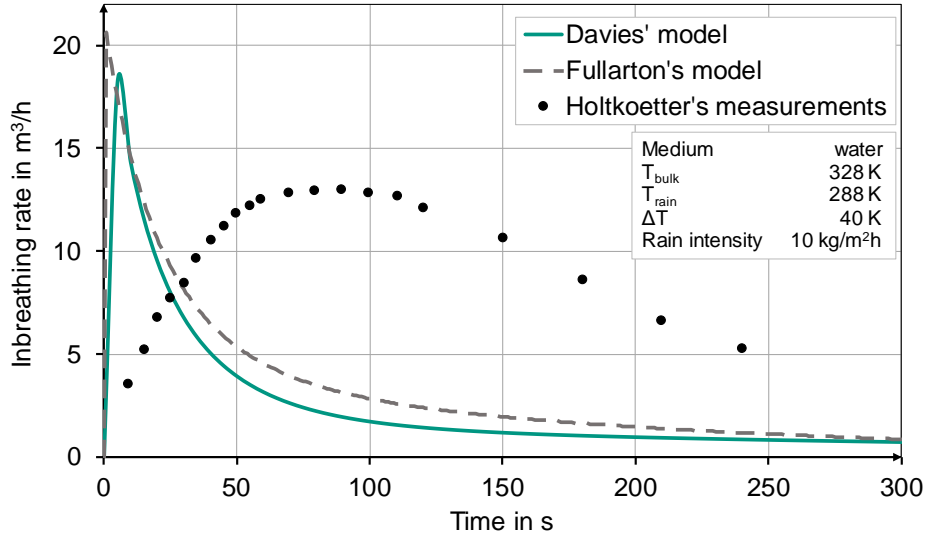


Figure 3. Inbreathing models of Davies (Moncalvo et al., 2016) and Fullarton (Fullarton et al., 1997) for condensable vapours compared to Holtkoetter's (Holtkoetter et al. 1997) measurements of water.

As to be seen from the figure, the calculated inbreathing volume flow rate is much larger than expected from the measurements. The deviation of the maximum inbreathing rate is at 55% with the Fullarton model and at 40% with the Davies model. The same calculations were performed with the medium methanol. With the Fullarton model, a deviation of 14% was noticed and a 5% underestimation with the Davies model, as depicted in figure 4. Regarding the time dependency, the maximum inbreathing rates were calculated right in the beginning whereby in the measurements the maximum rate was delayed by 90 seconds. As error analysis, two reasons seem to be obvious. The first one is related to the experimental conditions. The experimental conditions of Holtkoetter's measurements were not completely published and some assumptions were over taken from Abou-Chakra et al. (Abou-Chakra, 2016). The second reason is the occurrence of fog formation inside the tank that was observed by Holtkoetter and which is not included in Fullarton's and Davies' model. The formation of aerosols has a damping effect on the cooling process because condensation heat is released and therefore less condensate at the tank wall is formed. This effect causes a much lower maximum inbreathing rate and a widening of the curve. The intensity of this effect depends on the amount of fog that is formed.

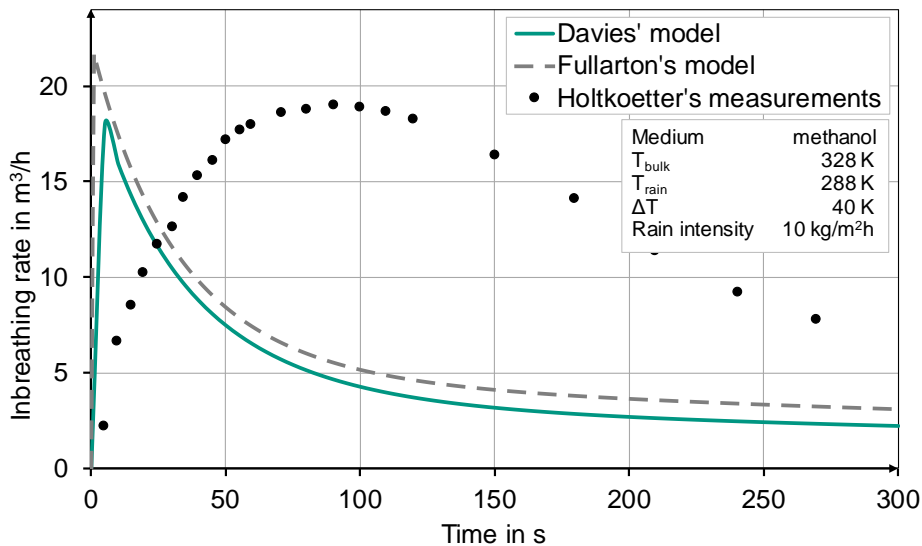


Figure 4. Inbreathing models of Davies (Moncalvo et al., 2016) and Fullarton (Fullarton et al., 1997) for condensable vapours compared to Holtkoetter's (Holtkoetter et al. 1997) measurements of methanol.

Since methanol forms less fog compared to water, the maximum inbreathing rate of the Holtkoetter measurements are more precisely predictable by literature models.

The validations of Fullarton's and Davies' model have shown that they are well qualified for inbreathing calculations with non-condensable gases for this particular measurement. For an accurate validation, a decent study on all measurements of Sigel is necessary. The comparison to the Holtkoetter's measurements demonstrated that the models are not valid for condensable vapours in small tanks, especially for stored media with high vapor pressure. It is questionable if the results are transferable to large tanks. A similar comparison to Holtkoetter's measurements was performed by Abou-Chakra et al. for the SuperChems Expert™ model. The SuperChems Expert™ model showed deviations of 1.7% with water vapor but 20% with methanol vapor (Abou-Chakra, 2016). A disadvantage of Fullarton's model is, that for the derivation of the mass balance the inbreathed air must be equal to the bulk phase, which is doubtful considering the temperature drop within sudden weather changes. If the air is assumed to be colder than the tank, the cooling process is accelerated. In Davies' model, the disadvantages of the temperature difference between the inbreathed air in the bulk phase was revised. The results show an improvement compared to Fullarton especially for gases with a low vapor pressure but without a satisfying solution. The Davies model is not always conservative, as the results in figure 4 have shown. Despite, the heat conduction through the condensate film is neglected in both models. For accurate sizing of compensation devices, it is necessary that the assumptions made within the calculation models are sufficiently conservative to prevent damage on the tank. Therefore, the heat transfer in particular is investigated in the CFD simulation in chapter 7.

6 Parameter Study on Inbreathing

For an evaluation of other impact factors, a parameter study with the model of Fullarton et al. (Fullarton et al., 1997) is performed. Therefore, a tank with a size of $2\,651\text{ m}^3$ is assumed, filled up with a vapor/air mixture of different compositions and with different media. Seven parameters are examined in total: the tank wall thickness, the tank geometry, the tank volume, the tank material, the rain intensity, the vapor proportion and the storage medium.

As result, obviously a thinner tank wall is beneficial for the heat transfer between the bulk phase and the environment so that a tank with a lower wall thickness cools down faster than a tank with a higher wall thickness. By varying the height to diameter ratio of the tank from 0.5 to 2 no remarkable deviations are noted. The discrepancy of inbreathing rates is less than 1%. In contrast, the tank volume has major impact on the inbreathing rate, see figure 5.

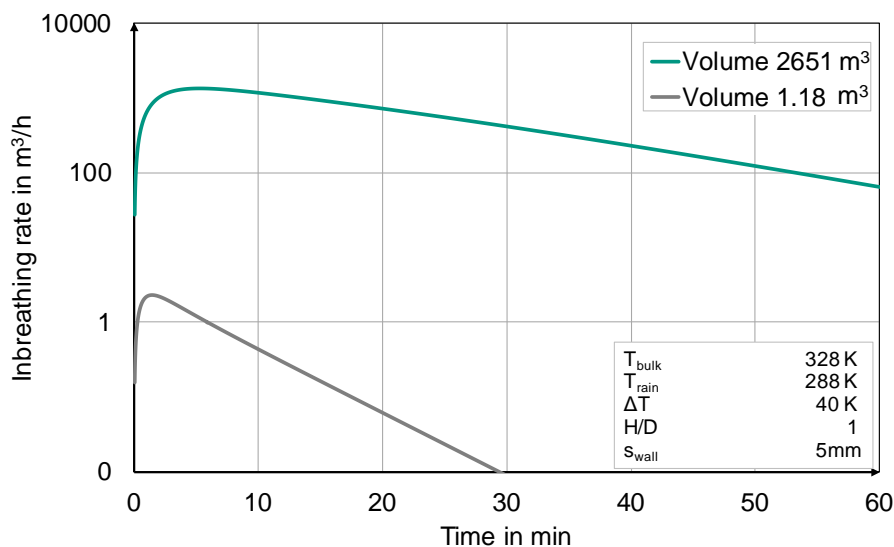


Figure 5. Inbreathing rates for a tank volume of $2\,651\text{ m}^3$ and 1.18 m^3 over time.

The inbreathing rate in the small tank increases and mitigates faster compared to the large tank. A reason for this behaviour is the faster cooldown of the small tank, see figure 6. Due to the poor heat transfer ability of gas, the volume of the large tank is cooled down very slowly, even though the wall temperature drops quickly in the beginning.

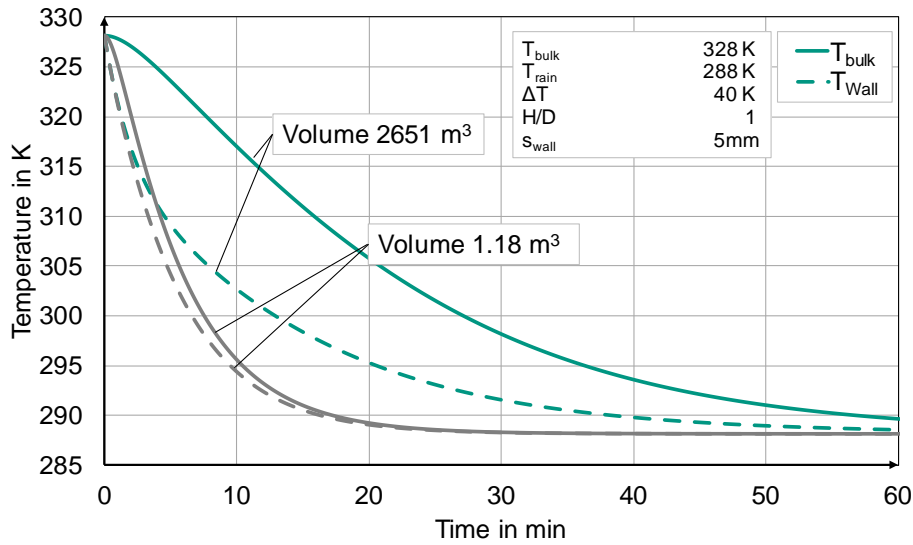


Figure 6. Wall and bulk temperature inside a storage tank with a volume of 2651 m³ and 1.18 m³ over time.

For an evaluation on the influence of the tank material, steel, stainless steel and steel concrete are compared. The inbreathing rates in the steel concrete tank is 17% higher compared to the other tanks, because of the slower cooldown of the concrete wall. As expected, the cooling process accelerates with increasing rain intensities and causes higher inbreathing rates, due to the faster decrease in temperature. With varying vapor content (11.8%, 50%, 100%) inside the tank, poor deviations of 6% are detected. As result, the influence of vapor content on inbreathing is negligible. A change of medium has a visible effect, as depicted in figure 7. The inbreathing rate is the highest for acetone and the lowest for water.

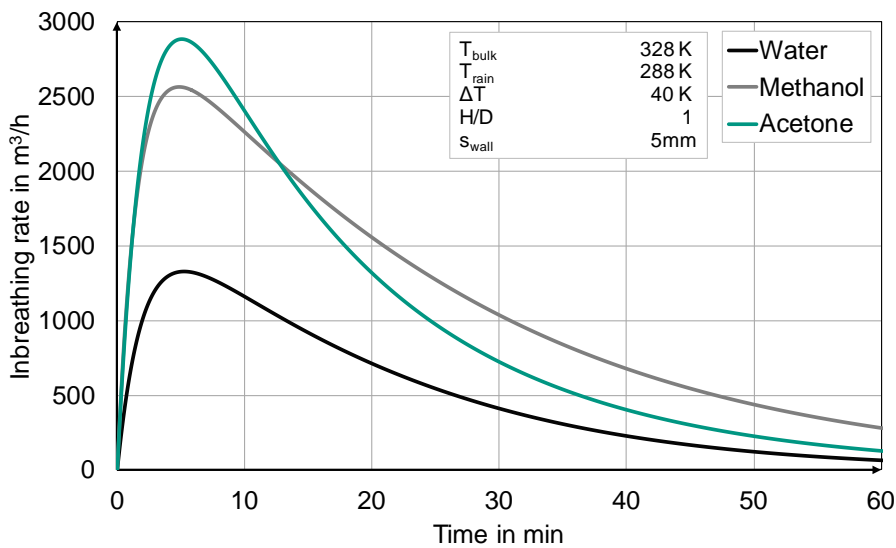


Figure 7. Inbreathing rates for acetone, methanol and water over time.

As mentioned by Holtkoetter et al. (Holtkoetter et al., 1997), homogeneous condensation is one impact factor on inbreathing. Due to the vapor pressure, acetone forms fog poorly compared to water and methanol which causes an increase in the inbreathing rate.

On the basis of this parameter study, some influences on inbreathing were pointed out. To receive a more accurate model, a detailed look on breathing phenomena with computational fluid dynamics (CFD) is necessary, considering location-dependent effects. In particular, the heat transfer simulation through the tank wall as first step to an overall calculation model is performed in the next chapter.

7 Simulation of Heat Transfer on a Storage Tank Wall

Breathing phenomena of low-pressure storage tanks have not been simulated with CFD yet. As a basis for a feasibility study for the further simulations in the ARTEM model, the two-dimensional (2D) cooling of a tank wall by heavy rainfall was performed with the *chtMuliregionFoam* solver of the OpenFOAM software, based on Sigel's measurements (Sigel et al., 1981). This solver uses the PIMPLE-Algorithm as a combination of PISO (Pressure Implicit with Splitting of Operator) and SIMPLE (Semi-Implicit Method for Pressure-Linked Equations) for the fluids with the following governing equations. A detailed description of the solver is outlined by el Abbassi et al. (el. Abbassi et al., 2017).

The mass transfer is described by:

$$\frac{\partial \rho}{\partial t} + \nabla \cdot (\rho w) = 0 \quad (8)$$

ρ is the fluid density and w the velocity of each phase. The momentum and energy transport are calculated with:

$$\frac{\partial \rho w}{\partial t} + \nabla \cdot (\rho w w) = -\nabla p + \nabla \left\{ \eta \left[\nabla w + (\nabla w)^T \right] \right\} - \nabla \left(\frac{2}{3} \eta (\nabla \cdot w) \right) \quad (9)$$

$$\frac{\partial \rho h}{\partial t} + \nabla \cdot (\rho w h) + \frac{\partial \rho K}{\partial t} + \nabla \cdot (\rho w K) - \frac{\partial p}{\partial t} = \nabla (a \nabla h) + \rho w g \quad (10)$$

Therein, p is the phase pressure, η is the dynamic viscosity of the fluid, h is the specific enthalpy of the fluid, a is the thermal diffusivity and the kinematic energy K is calculated with:

$$K = \frac{w^2}{2} \quad (11)$$

The system of equations is solved for both fluids, while the bulk phase is compressible and the liquid phase is incompressible. In both fluids a laminar flow condition is assumed. In the solid phase, only the energy equation has to be solved which is described by Fourier's law:

$$\frac{\partial \rho h}{\partial t} = \nabla (a \nabla h) \quad (12)$$

The heat transfer between the phases is coupled with the assumption that the temperature between the solid and the fluid phases at the interface is equal. Furthermore it is assumed, that the heat flux entering one region at one side of the interphase is equal to the heat flux leaving the other region in the other side of the domain.

The setup for the two-dimensional (2D) cooldown of the tank wall is shown in Figure 8, including the rain film of a constant width and the boundary layer of the bulk phase. The height of the simulated system is 10.6 m considering atmospheric pressure. As the aim of the study is to investigate the heat transfer through the tank wall, the bulk phase has a relatively small width of 430 mm to save computation time. The initial temperature of the bulk was 306.5 K. For top and bottom, an inlet-outlet boundary condition for velocity and temperature is assumed. From the bulk phase to the wall, a no slip condition is applied. The tank wall, with a width of 5 mm has the initial temperature of the bulk phase and a zero-gradient boundary condition for temperature on top and bottom. The rain film has a constant width of 2 mm over the height of the tank, an initial temperature of 287.5 K and an initial velocity of 0.37 m/s at the inlet at the top. The velocity was calculated with the Reynolds approach due to the assumption of a constant rain intensity of 65 kg/m²h. On the bottom, the inlet-outlet boundary condition is applied.

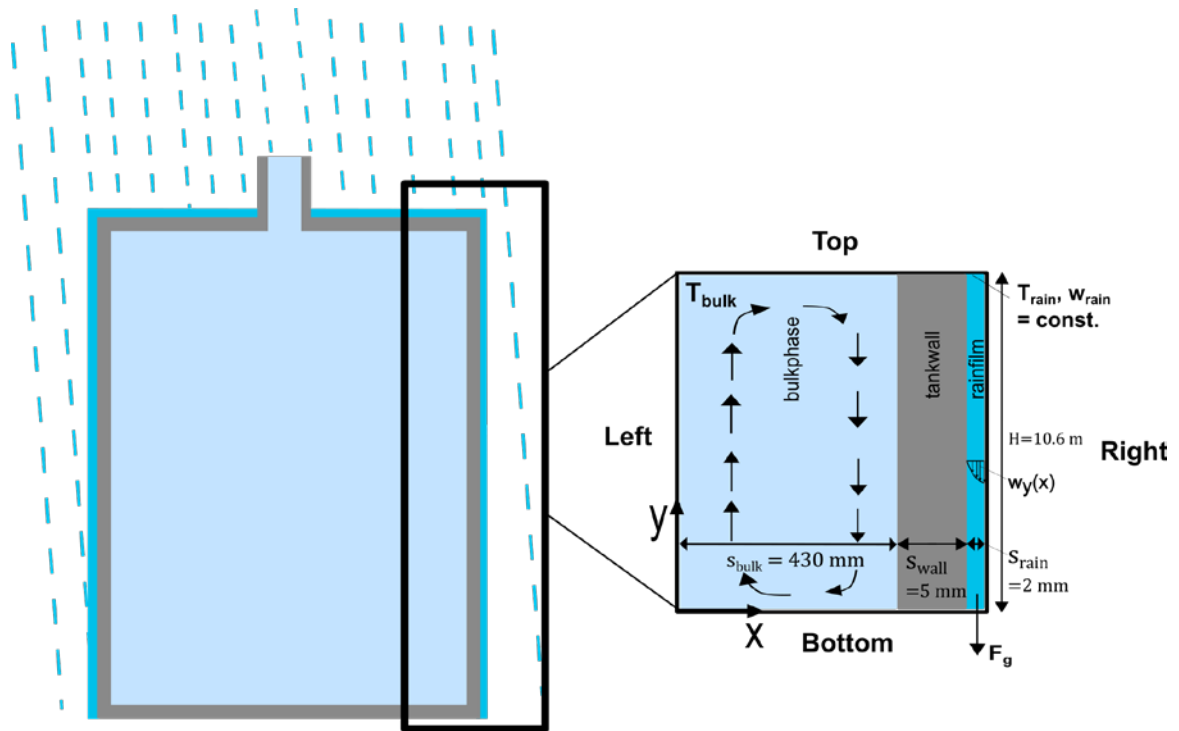


Figure 8. Simulation setup.

On purpose of saving calculation time, a grid study on a small section of 0.5 m height was performed. The results are depicted in Figure 9 and 10.

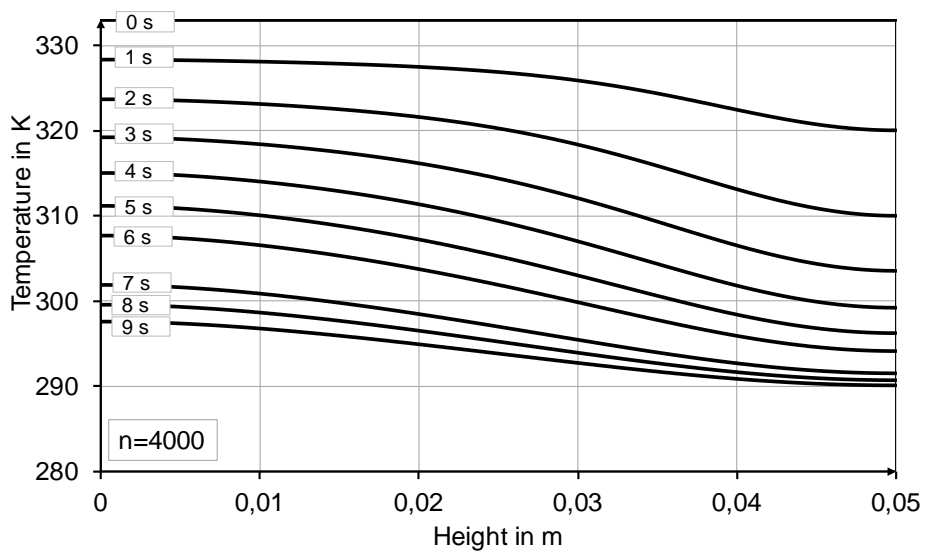


Figure 9. Temporal cooldown of the wall surface inside the tank over the tank height.

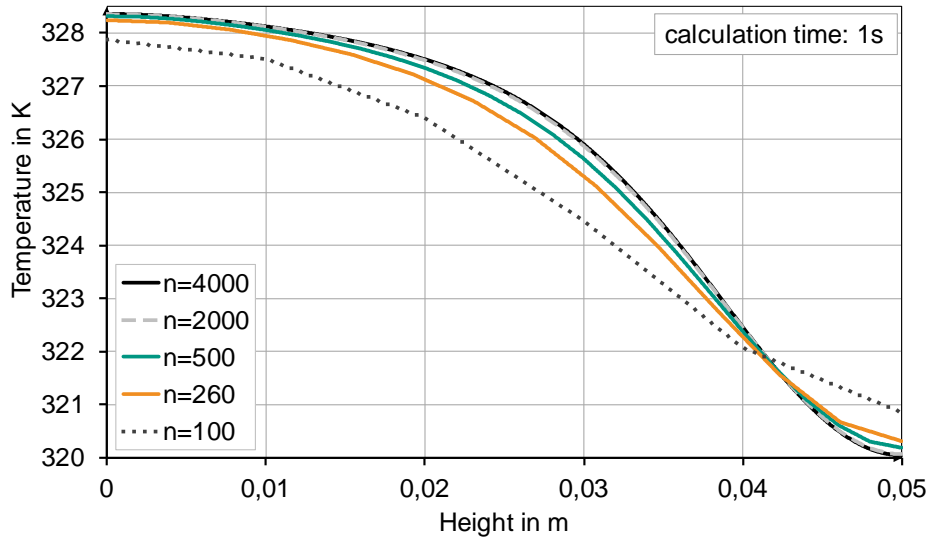


Figure 10. Grid study on the cooldown of the wall surface over the tank height at a simulation time of 1 s.

The grid study was performed using 100 cells per meter in x-direction and varying 4000 to 100 cells per meter in y-direction. The maximum deviation between 4000 cells and 100 cells is 1.51 K that corresponds to 0.46%. For further calculations of the heat transfer between bulk, wall and rain, the number of grid points in y-direction was set to 260 cells per meter what complies with an error of 0.19%.

The focus of the simulation is on the calculation of the heat transfer coefficient between bulk and wall and rain. In figure 11 the development of the heat transfer coefficients between the bulk, the wall and the rain are displayed.

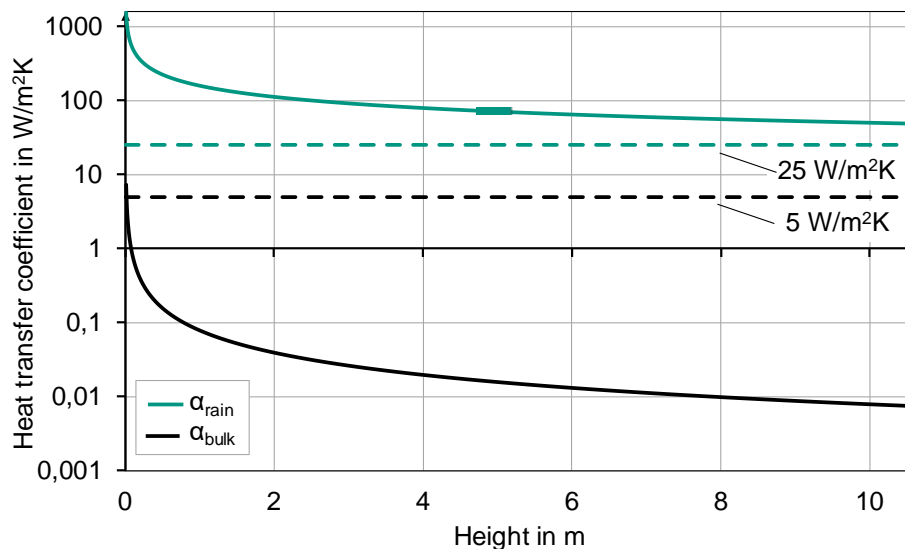


Figure 11. Heat transfer coefficients of rain, bulk and the tank wall over the tank height.

As expected, the heat transfer from the rain film to the ambience is slightly higher than in the bulk phase. Starting at $1565 \text{ W/m}^2\text{K}$ at the tank bottom, the heat transfer coefficient decreases to $48 \text{ W/m}^2\text{K}$ on the top. Literature models assuming a heat transfer coefficient of $25 \text{ W/m}^2\text{K}$ (Fullartion et al., 1987, Moncalvo et al., 2016), underestimate heat transfer by 48%. In the bulk phase, the heat transfer coefficient starts at $7 \text{ W/m}^2\text{K}$ and drops to $0.007 \text{ W/m}^2\text{K}$. With a condensation film on the inside of the tank, the heat transfer from the bulk to the condensation film is on the same scale as the heat transfer coefficients at the outer surface and the heat flux increases. Considering heat conduction through the film, the heat flux is even higher. Therefore, it is questionable if the assumption of a heat transfer coefficient of $5 \text{ W/m}^2\text{K}$ (Fullartion et al., 1987, Moncalvo et al., 2016) and the neglect of the heat conduction through the condensate film is always conservative.

On heat conduction, further investigation is needed in future work. Subsequent these simulations will be extended with a pressure gradient from the depression of the weather change and the emptying and filling process of tanks.

8 Conclusion and Outlook

The results have shown, that many phenomena regarding inbreathing of storage tanks have neither been considered in common calculation models nor in the standards. As this study and the research of multiple authors of (Fullarton et al., 1987, Holtkoetter et al., 1997, Moncalvo et al., 2016) demonstrate, condensation has a major impact on the inbreathing volume flow rate. The models in the standards (API 2000 - American Petroleum Institute, 2014 or DIN EN ISO 28300 - Deutsches Institut fuer Normung, 2012) are derived for non-condensable tank content and are therefore not conservative or applicable to tanks containing condensable vapours.

A large disadvantage of the literature models is, that the condensation mass flux is included in the mass balance though, but the heat transfer is calculated with the assumption of a dry wall by considering a heat transfer coefficient of $5 \text{ W/m}^2\text{K}$ and a neglect of heat conduction (Moncalvo et al., 2016 and Fullarton et al., 1984). For non-condensable gases in the tank, this assumption is sufficiently conservative, as to be seen from figure 11, black line. For condensable vapours the heat transfer coefficient is increased considering a condensation flow at the tank wall. The heat transfer is then in the same magnitude as the rain film in figure 11, green line. Film dynamics like the shape of the film, flow effects or heat conduction might increase the heat flux through the tank wall significantly und shall therefore be investigated in further studies. In Fullarton's model, the assumption of equality between the bulk and ambience temperature in the mass balance seems to be unrealistic when it comes to sudden weather changes.

Film condensation but also fog formation has major impact on inbreathing as shown in figure 2 and 3 and the work of Holtkoetter et al. (Holtkoetter et al., 1997) for small laboratory equipment of 1.18 m^3 . The transferability of the assumptions and observations to large storage tanks has to be verified in prospective measurement campaigns. Thus, further investigation on the entrainment of inbreathed air and turbulence effects causing local non-equilibrium in the bulk phase is needed, to understand the promotion of fog formation inside the tank. The governing effect of heterogeneous condensation due to particles in the inbreathed air is not yet considered and should be taken into account. Thus, with the information given in Holtkoetter and Sigel, it is hardly possible to simulate the measurement conditions, accurately, because of many uncertainties and inconsistencies. Therefore, new measurement campaigns are necessary.

All models mentioned above are derived for single components, predominantly water and air. In industry, liquids like naphtha, gasoline or other multi components are stored in those tanks. The impact of mixing properties on inbreathing and the transferability to common breathing models needs to be validated. Currently there is no multi component model published in literature. The influence of those effects shall be verified in subsequent models.

All the different conditions of breathing will be coupled as overall model in the new CFD approach ARTEM (advanced reactor and storage tank emission model). Regarding the overall model, some inbreathing phenomena, e.g. the boundary layer at the tank wall, drops and particles inside the tank or the rain film on the outer surface, cannot be resolved in sufficient detail on purpose of computational costs. Therefore, a multi scale approach must be developed to enable the coupling of the phenomena described in chapter 2. The model is currently under development and will be validated with especially designed measurements on a storage tank with a volume of 200 m^3 . Lastly, the environmental aspects, like the formation of a rain film, wind flow and other local aspects need to be defined in a standardized way for a reliable and detailed modelling of breathing phenomena.

Acknowledgements

We would like to thank the Braunschweiger Flammenfilter GmbH for funding this research project. In addition, we would like to thank Markus Stueven and Kathi Heithausen for supporting the work within their master theses.

Nomenclature

A	$[\text{m}^2]$	tank shell surface
a	$[\text{m}^2/\text{s}]$	thermal diffusivity
$c_{p_{cond}}$	$[\text{J}/\text{kgK}]$	specific heat capacity condensate
$c_{p_{wall}}$	$[\text{J}/\text{kgK}]$	specific heat capacity tank wall

$c_{p,air}$	[J/kgK]	specific heat capacity air
$c_{p,vap}$	[J/kgK]	specific heat capacity vapor
F_g	[N]	gravity force
\dot{H}_{air}	[J/s]	enthalpy flux air
\dot{H}_{cond}	[J/s]	enthalpy flux film condensate
$\dot{H}_{cond,sp}$	[J/s]	enthalpy flux fog
H / D	[-]	height to diameter ratio of the tank
h	[W/m ²]	specific enthalpy of the fluid phase
K	[m ² /s ²]	kinetic energy of the fluid phase
k_{in}	[W/m ² K]	heat transfer coefficient bulk to wall
M_{air}	[kg]	air mass inside the tank
M_{cond}	[kg]	film condensate mass
$M_{cond,sp}$	[kg]	fog mass
M_{vap}	[kg]	vapor mass inside the tank
p	[Pa]	pressure in the fluid phase
$Q_{v,air}$	[m ³ /hr]	inbreathed air volume flow rate
$Q_{v,cond}$	[m ³ /hr]	film condensate volume flow rate
$Q_{v,cond,sp}$	[m ³ /hr]	fog volume flow rate
\dot{Q}_{out}	[J/s]	heat flux from bulk to wall
s_{bulk}	[K]	bulk thickness in the CFD simulation setup
s_{rain}	[K]	rain film thickness
s_{wall}	[K]	tank wall thickness
T_{amb}	[K]	ambient temperature
T_{bulk}	[K]	bulk temperature
T_{cond}	[K]	condensate temperature
T_{rain}	[K]	rain temperature
T_{wall}	[K]	tank wall temperature
t	[s]	time
U_{bulk}	[J/s]	bulk internal energy
V_{bulk}	[m ³]	bulk volume
w	[m/s]	rain film velocity
x, y, z	[m]	directions of the coordinate system
$\Delta h_{v,cond}$	[J/kg]	specific vaporisation enthalpy of the condensate
α_{air}	[W/m ² K]	heat transfer coefficient from bulk to the tank wall
α_{rain}	[W/m ² K]	heat transfer coefficient from rain film to the ambience
ρ_{air}	[kg/m ³]	density of air
ρ_{cond}	[kg/m ³]	density of the condensate
η	[Pa s]	dynamic viscosity

References

- el Abbassi, M. ; Lahaye, D. J. P.; Vuik, C.: *Modelling turbulent combustion coupled with conjugate heat transfer in OpenFOAM*, Conference Paper from MCS 10, Neaple, Italy (2017).
- Abou-Chakra, D.: *Dynamic Modeling of Inbreathing Requirements for Low-Pressure Storage Tanks*, Master of Science, Northeastern University, Boston, Massachusetts, (2016).
- American Petroleum Institute: *Venting Atmospheric and Low-pressure Storage Tanks. API STANDARD 2000* (2014).
- Cronin, K. and Davies, M.: Analysis of the variability in collapse time of a process storage vessel due to internal steam condensation. *Proceedings of the Institution of Mechanical Engineers, Part E: Journal of Process Mechanical Engineering*, vol. 222, no. 3 (2008), pp. 171–181.
- DIN Deutsches Institut für Normung e. V.: *Erdoel-, petrochemische und Erdgasindustrie – Be- und Entlüftung von Lagertanks mit atmosphärischem Druck und niedrigem Ueberdruck (ISO/DIS 28300:2011). Deutsche Fassung EN ISO 28300:2011 (Februar 2012)*, no. 28300.
- Ennis, T.: Pressure relief considerations for low-pressure (atmospheric) storage tanks. *ICHEME Symposium 151*, (2006).
- Foerster, H., Schampel K., and Steen H.: *Atmungsvorgänge infolge von Witterungseinflüssen an Lagertanks für brennbare Flüssigkeiten. Physikalisch Technische Bundesanstalt (Technical Report)*, (1984).
- Fullarton, D.: Sicherheitstechnische Ueberlegungen bei Atmungsvorgängen in Lagertanks - Einfluß der Kondensation von Produktdaempfen. *Chemie Ingenieur Technik*, vol. 58, no. 1 (1986), pp. 38–40.
- Fullarton, D.; Evripidis, J. and Schluender, E.U.: Influence of product vapour condensation on venting of storage tanks. *Chemical Engineering and Processing: Process Intensification*, vol. 22, no. 3 (1987), pp. 137–144.
- Goßlau, W.; Mueller, E.; Weyl, R.: *Thermodynamische Grundlagen der Behälteratmung aufgrund von Witterungseinflüssen,* *Technische Ueberwachung*, vol. 1, no. 26 (1985), pp. 16–22.
- Holtkoetter, T.; Shang, J. and Schecker, H.-G.: *Behälteratmung - Experimentelle Untersuchungen und Entwicklung eines Vorhersagemodells. Chemie Ingenieur Technik*, vol. 69, no. 3 (1997), pp. 361–366.
- ioMosaic Corporation, *SuperChems Expert™ component of Process Safety Office™*, (2015).
- Moncalvo, D.; Davies, M.; Weber, R. et al.: Breathing losses from low-pressure storage tanks due to atmospheric weather change. *Journal of Loss Prevention in the Process Industries*, vol. 43 (2016), pp. 702–705.
- Salatino, P.; Volpicelli, V. and Volpe, P.: On the Design of Thermal Breathing Devices for Liquid Storage Tanks. *Process Safety and Environmental Protection*, vol. 77, no. 6 (1999), pp. 354–359.
- Sigel, R.: *Auswertung der Tankabkühlungsversuche 1980 und 1981 im Werk Höchst. Technical Report (Hoechst AG)*, (1980).
- Sigel, R.; Schwarz, H., Kuxdorf, B. et al.: *Maximaler Volumenstrom bei der Abkuehlung von Festdachtanks. Technical Report (Hoechst AG)*, (1981).
- Sigel, R.; Schwarz, H.; Kuxdorf, B. et al.: *Praktische und theoretische Untersuchung der Beatmung von Festdachtanks. Chemie Ingenieur Technik*, vol. 55, no. 5 (1983), pp. 377–379.

Address: Natalie Schmidt, M.Sc; CSE Center of Safety Excellence gGmbH, Joseph-von-Fraunhofer-Straße 9, 76327 Pfinztal, Germany
email: natalie.schmidt@cse-institut.de

Prof. Dr.-Ing. Jens Denecke, CSE Center of Safety Excellence gGmbH, Joseph-von-Fraunhofer-Straße 9, 76327 Pfinztal, Germany
email: jens.denecke@cse-institut.de

Prof. Dr.-Ing. Juergen Schmidt, CSE Center of Safety Excellence gGmbH, Joseph-von-Fraunhofer-Straße 9, 76327 Pfinztal, Germany
email: juergen.schmidt@cse-institut.de

Dr.-Ing. Michael Davies, Braunschweiger Flammenfilter GmbH, Industriestr. 11, 38110 Braunschweig, Germany
email: michael.davies@protego.com